STABILITY OF BOOMED SPACECRAFT CONFIGURATIONS DURING ATMOSPHERIC DIPPING CAMPAIGNS

Dr. Joseph R. Schultz
University of Maryland - College Park

ABSTRACT

This paper discusses several stability results on the stability of aeromaneuvering, flexible spacecraft. The fields of spacecraft aeromaneuvering, flexible spacecraft dynamics, and rarefied gas flows are connected to understand the dynamics of flexible spacecraft as they travel through the upper atmosphere. Insightful analytic stability solutions were developed to help a spacecraft builder design a stable spacecraft. Boom flexibility plays an important role in dynamic stability, but the effect of flexibility will depend on the boom's orientation and positioning. The solutions can also be used to produce design maps that are useful when tracking stability as the parameters change over the lifetime of the mission. The work has direct application to the boomed NASA GEC spacecraft. The work shows that its booms should be placed as far back on the spacecraft as possible for the greatest stability. Making the booms more rigid will also help the stability in the yaw plane, but diminishing returns are seen after a certain level of stiffness.

INTRODUCTION

Most satellites and spacecraft fly in high enough orbits so that they will not experience significant aerodynamic drag in an orbital time period. However, there are some missions where a spacecraft may wish to enter the upper regions of the Earth's atmosphere for a short period of time. These missions may be operational or scientific in nature, such as to conduct an aeroassist for an orbital plane change or to take magnetosphere readings in the upper atmosphere.

In some cases, these spacecraft may have large flexible booms. Booms may be used for solar panels, antenna, or to hold scientific instruments away from the spacecraft's body. An important engineering and design question is determining how large, flexible booms affect the overall stability of the spacecraft during the atmospheric portion of flight.

Much of the literature on aeromaneuvers focuses on spacecraft with space-shuttle-like configurations where the spacecraft is treated as a point-mass model.[1] Because of the rigid-body nature of these spacecraft, internal flexibility modes are usually not of concern. Spacecraft with long, flexible booms, however, present an extra layer of dynamics. Even in free-space, instabilities may arise that would not normally be predicted by a point-mass model. Although the literature quite extensively covers the dynamics and control of flexible spacecraft in free-space,[2,3] there is little analysis when those types of spacecraft undergo the aerodynamic effects of an atmospheric passage. A connection needs to be made between flexible spacecraft dynamics and aeromaneuvering to understand how a spacecraft behaves under these conditions.

Such a connection is important for spacecraft missions currently under development. The Geospace Electrodynamics Connections Mission (GEC)[4] spacecraft, currently being designed by the National Aeronautics and Space Administration (NASA) at the Goddard Space Flight Center, is a key example of a flexible spacecraft undergoing a shallow atmospheric pass. The spacecraft has six long booms that hold instruments to measure the local electric and magnetic fields. An illustration of the spacecraft is shown in Fig. 1. One of the key missions of the spacecraft is to dip into the upper atmosphere (approximately 130 km above the Earth's surface) to take field readings at those altitudes. In this rarefied atmospheric region there will be significant

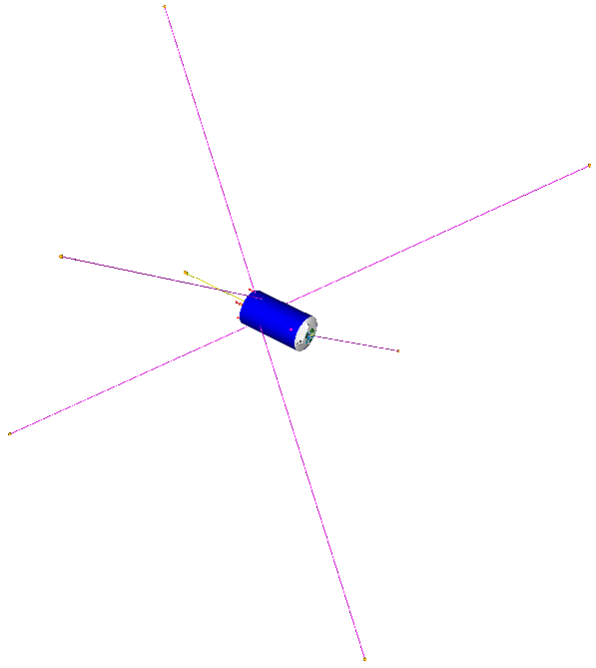

Fig. 1: GEC Spacecraft[4]

aerodynamic loading on the booms and spacecraft. The key concern is that the booms may cause instabilities that lead to the loss of the spacecraft.

Understanding the dynamics and preventing instabilities are important research goals that need to be accomplished. The research needs to answer the following questions:

- How do the placement of the booms and the location of the aerodynamic center of the spacecraft affect the stability results?
- How does boom flexibility affect stability?
- What are the stable spacecraft configurations?

These are important questions because there have been many previous spacecraft that have experienced costly stability problems[5] even without aerodynamic effects. Adding aerodynamic effects to the flexible spacecraft will only augment the likelihood of stability problems. Future designers of aeromaneuvering, flexible spacecraft must account for these effects.

AERODYNAMIC MODEL

The most important element in investigating how a flexible spacecraft performs during aeromaneuvering is how the flexible spacecraft surfaces interact with the atmosphere. The main driver that determines the aerodynamics of this interaction is the atmospheric or gas-surface interaction model.

There are two main types of aerodynamic models available: a continuum model or a discrete particle or molecular model. The Knudson number will determine which type of aerodynamic model to use. The Knudson number is the ratio of the molecular mean free path to the spacecraft length:

$$Kn = \frac{\lambda}{L^*} \tag{1}$$

For small Knudson numbers, the molecules will have significant interaction with each other before and after hitting the spacecraft surface. For large Knudson numbers, essentially the molecules do not interact with each other before or after hitting the spacecraft surface, thus the molecules can be treated independently and only momentum transfer needs to be considered.

Generally, if the Knudson number is greater than 1, a rarefied aerodynamic model should be used. If the Knudson number is much, much less than 1, a continuum aerodynamic model can be used[6]. For Knudson numbers between 0.1 and 1, a transitional model might be required.

At very low atmospheric densities, the mean free path is large, so for most spacecraft making very shallow dips into the atmosphere, a rarefied gas-surface model can be used. The lowest altitude this assumption is valid for depends on the mean free path. For a spacecraft that is 3-5 meters long, a rarefied model will be valid for altitudes down to 120-125 km[7]. Since this work concentrates on spacecraft excursions above these altitudes, a rarefied aerodynamic model is appropriate.

Rarefied Gas-Surface Interaction Model

For simplicity, a modified Maxwellian rarefied gas-surface model will be used to calculate the lift and drag forces on the spacecraft surfaces. The Maxwell model[8] states that molecules will either reflect diffusely from a surface with complete energy accommodation or will reflect specularly with no change in energy.

By considering a full range of momentum accommodation, ε ($\varepsilon = 0$: molecules "hit-and-stick" to the surface; $\varepsilon = 1$: molecules reflect from the surface with the same momentum they arrived with), and fraction of specular to diffuse behavior, ξ ($\xi = 0$: complete diffuse behavior; $\xi = 1$: complete specular behavior), the entire range of gas-surface interactions can be modeled for aerodynamic force determination.

A modified form of the Maxwellian model has been previously derived by Lewis[9] and Bowman[10], and they provide formulas for lift and drag. By converting their equations into the standard notation of:

$$L = \frac{1}{2}\rho V_o^2 S^* C_L \qquad D = \frac{1}{2}\rho V_o^2 S^* C_D \tag{2), (3}$$

the lift and drag coefficients for a flat surface can be written as:

$$C_{Dspec/flat} = 2\left(\sin\alpha + \frac{\bar{c}}{4V_o}\right)(1 - \varepsilon\cos 2\alpha) \qquad C_{Lspec/flat} = 2\left(\sin\alpha + \frac{\bar{c}}{4V_o}\right)\varepsilon\sin 2\alpha \tag{4), (5}$$

$$C_{Ddiff/flat} = 2\left(\sin\alpha + \frac{\bar{c}}{4V_o}\right)\left(1 + \varepsilon\frac{2}{3}\sin\alpha\right) \qquad C_{Ldiff/flat} = 2\left(\sin\alpha + \frac{\bar{c}}{4V_o}\right)\varepsilon\frac{2}{3}\cos\alpha \tag{6), (7}$$

$$C_D = \xi C_{Dspec} + (1-\xi)C_{Ddiff} \qquad C_L = \xi C_{Lspec} + (1-\xi)C_{Ldiff} \tag{8), (9}$$

where α is the angle between a spacecraft surface and the incoming flow, and $\bar{c}/V_o$ is the molecular thermal speed ratio.

The benefits of this model are that the equations are simple and concise, relying on only a few parameters to determine the lift and drag. The more detailed Nocilla or Cercignani-Lampis model, or Direct Simulation Monte Carlo (DSMC) analysis could also be used, but since the net lift and drag are the only needed values and a detailed flow description is not required, this modified Maxwellian model is sufficient and simplest to use.

Drag and Lift of the Spacecraft

Spacecraft Body

Eqs. (2) - (9) for the lift and drag are only for a flat surface. To find the overall lift and drag coefficients for a complex spacecraft surface, the same equations can be used, but the spacecraft surface needs to be approximated by a group of flat plates. With this panel method, the lift and drag could be calculated over each surface of the body and the results averaged to provide the overall lift and drag coefficients. Bowman[11] provides some detail for such a method.

For some spacecraft shapes, the lift and drag equations can be integrated over a spacecraft surface instead of using a panel method. If the integration is feasible, an analytic solution can be found that is more accurate and may be preferable to a panel method solution. These solutions are generally only found for simple, smooth spacecraft shapes. This technique has been used by Sentman[12] for several simple spacecraft body shapes.

Spacecraft Booms

Not only is it important to calculate the lift and drag of the spacecraft body, it is also necessary to calculate the lift and drag of the spacecraft's booms. If the booms are flat in nature, similar to a flat wing, solar panel, or deployed out like a tape measurer, the lift and drag of the booms can be calculated from Eqs. (2) - (9) where α is the angle the booms make with the incoming flow. The assumption is that only one side of a flat boom is seen by the flow.

If the spacecraft's flexible booms are of a complex shape a panel method or integration technique may need to be used to calculate the lift and drag. Schultz[13] has shown, however, that under expected rarefied flow conditions where the accommodation fraction and thermal speed ratio are small, and especially when the interaction is diffuse, a complex boom shape can be approximated by a flat plate. Therefore, a flat plate boom model will be used in the following analysis.

LINEAR BOOM MODEL

During the spacecraft's flight through the upper atmosphere, the spacecraft's booms will bend under the aerodynamic load. This aeroelastic interaction can be complex with non-linear internal stresses and non-linear aerodynamic forces along the length of the boom. However, if one linearizes this aeroelastic system, important physical quantities can be determined which capture the most important parts of the system.

The bending beam system can be linearly reduced to a rigid boom connected to the spacecraft body by a torsional spring. This linear system is illustrated in Fig. 2. The linear system will be able to capture the tip deflection amount and the first mode of vibration.

The boom is set at an angle of attack of θ_o, but the oncoming flow will bend the boom an additional amount θ. This θ is the deflection angle. The resulting angle of the boom with respect to the flow is:

$$\phi = \theta_o + \theta \tag{10}$$

So, assuming θ is small, the boom's lift and drag coefficients can be written in linear form as:

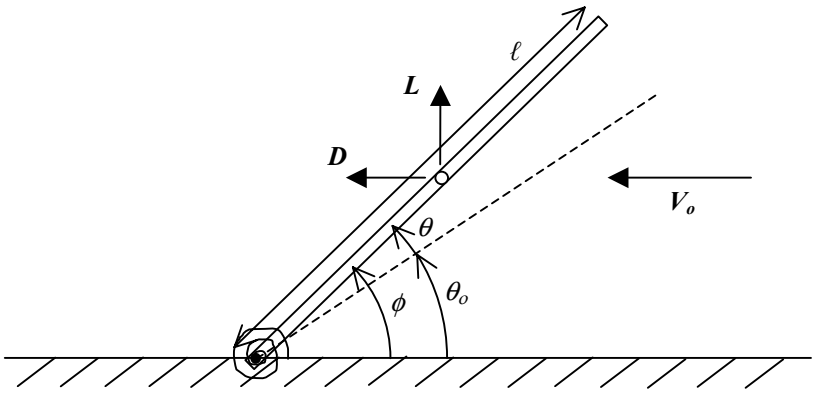

Fig. 2: Boom in a Flow

$$C_L = C_{Lo} + C_{L\alpha}\theta \qquad C_D = C_{Do} + C_{D\alpha}\theta \tag{11), (12}$$

where these coefficients are calculated (for flat booms) from Eqs. (2) - (9) at $\alpha = \theta_o$:

$$C_{Lo} = C_L\big|_{\alpha=\theta_o} \qquad C_{Do} = C_D\big|_{\alpha=\theta_o} \qquad C_{L\alpha} = \frac{\partial C_L}{\partial \alpha}\bigg|_{\alpha=\theta_o} \qquad C_{D\alpha} = \frac{\partial C_D}{\partial \alpha}\bigg|_{\alpha=\theta_o} \qquad (13)\text{ - }(16)$$

Note: this method will also work for any shape boom as long as a linear Lift and Drag profile can be determined as in Eqs. (11) and (12).

EQUATIONS OF MOTION

A two-dimensional, linear spacecraft model will be developed. Such a model provides a reasonable estimate of the dynamic behavior of the spacecraft. The spacecraft model will then be used as the basis for creating the equations of motion. The benefits and limitations of the model will be discussed throughout this section.

Spacecraft Model

The spacecraft model consists of several rigid bodies with one being the main spacecraft body (body *B*) and the others being any number of booms (bodies A_n) attached to body *B* at various locations (points O_n). This common configuration is often called a "hub-arm" configuration. Fig. 3 shows a model of the spacecraft. For simplicity, only two booms are shown.

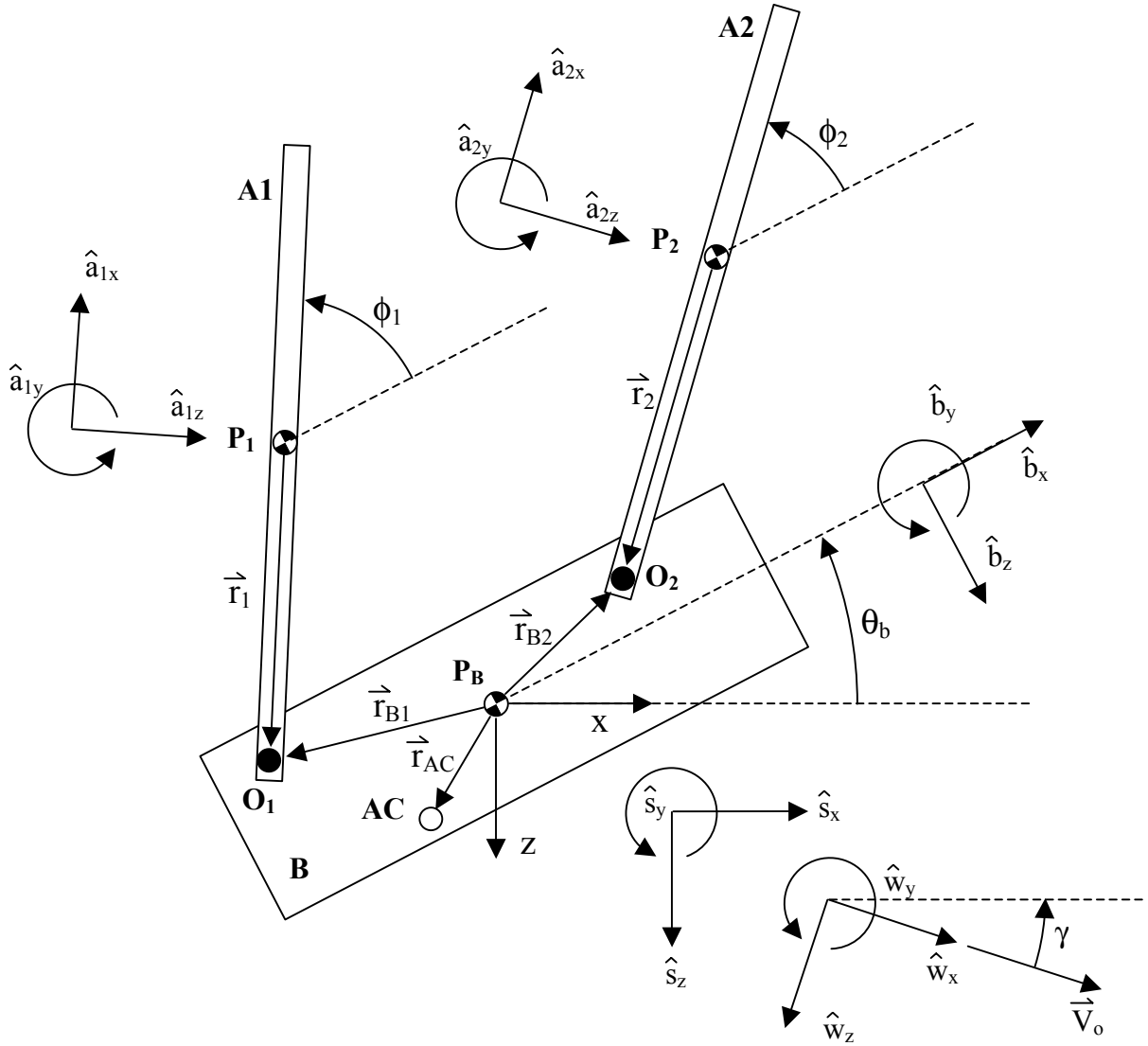

Fig. 3: Spacecraft Model

Several frames of reference are shown with the model. The '*b*'-frame is the spacecraft body frame, the '*s*'-frame is the spacecraft's orbit frame, the '*w*'-frame is the wind-frame, and the '*a*'-frames are each spacecraft arm's frame. Commonly, the $\hat{s}_x$ -direction is called the along-track orbit direction and $\hat{w}_x$ -direction is called the in-track orbit direction.

Equation Development

Separation of Spacecraft and Orbit Stability

To take advantage of classic stability and control analysis techniques, linearized equations of motion will be developed. The largest difficulty in this approach is to handle one of the major components of the aerodynamics, density, because it will vary exponentially with the orbit height of the spacecraft. Any linearization of the density as a variation of height will cause large errors when predicting the flight path of the satellite.

However, if one limits the discussion to a study of the dynamics of the spacecraft itself and not on the stability of maintaining specific orbit paths, then a solution where density is held as a constant can be used. Later, when one knows that a particular spacecraft configuration meets the designer's particular stability needs, it is possible to move to a non-linear or point-mass model such as one by London[14] or Vinh[15] to evaluate the flight path requirements. It is likely that several of these iterations may be done during the entire design process.

Flat-Earth Model

To investigate the dynamic behavior of the spacecraft across the entire flight regime, "snapshots" at various altitudes (densities) can be taken. Of greatest interest is the altitude where the aerodynamics will have the greatest effect. This occurs at the spacecraft's perigee where it is at the bottom of its atmospheric dip. It is here where the dynamics are the most interesting, and it is here where all of the following analysis will take place. At the perigee point, the spacecraft's trajectory can be approximated as straight and level at a constant altitude. At this point of level flight, a flat-Earth dynamic model can be used without loss of detail.[16] Assuming a flat-Earth model in this manner, the gravity force is implicitly omitted in the equations of motion.

2-D Model

The spacecraft of interest in this work are not spin stabilized. Because the spacecraft isn't spinning (and due to the symmetric nature of the space vehicles that will be examined), the motion won't be coupled between different planes. Therefore a 2-D model of the spacecraft is acceptable and the dynamics of the spacecraft can be examined for each plane independently.

Structural Modeling of the Booms

The booms will be modeled as rigid bodies connected to the main body by a linear, torsional spring. The torsional spring is assumed to be linear, so that the moment on the spring depends on the deflection angle and angular velocity through the spring constant k' and damping constant b':

$$M = -k'\theta - b'\dot{\theta} \tag{17}$$

This will capture the first mode of vibration in the dynamics.

Aerodynamic Force Modeling

It will be assumed that the flight path of the spacecraft will be confined to an altitude of at least 125 km above the Earth's surface and higher in order to minimize drag and large heating rates. At these altitudes, a rarefied gas-surface interaction model will be needed as previously described. The linearization of the boom's lift and drag terms in Eqs. (11) and (12) will be used.

It will also be assumed that the aerodynamic force will be the dominant force acting on the spacecraft.

Spacecraft Equation of Motion

For simplicity, a spacecraft with only two booms will be derived. Once the equations of motion are generated for a two-boom spacecraft, the form of the equations will be readily apparent for a spacecraft with any number of booms.

The equations of motion are in the standard form of:

$$M\dot{\vec{u}} = C\vec{u} + K\vec{q} + \vec{f} \tag{18}$$

where $\vec{u}$ and $\vec{q}$ are arrays of generalized velocities and generalized coordinates:

$$\vec{u} = [u_1 \quad u_2 \quad u_3 \quad u_4 \quad u_5]^T \qquad \vec{q} = [q_1 \quad q_2 \quad q_3 \quad q_4 \quad q_5]^T \tag{19) - (20}$$

Referring to Fig. 3, a convenient choice of generalized velocities and generalized coordinates are:

$$q_1 = \frac{x - V_o t}{R_o} \qquad q_2 = \frac{z - R_o}{R_o} \qquad q_3 = \theta_b \qquad q_4 = \theta_1 \qquad q_5 = \theta_2 \tag{21a) - (21e}$$

$$u_1 = \frac{\dot{x} - V_o}{V_o} \qquad u_2 = \frac{\dot{z}}{V_o} \qquad u_3 = \dot{\theta}_b \qquad u_4 = \dot{\theta}_b + \dot{\theta}_1 \qquad u_5 = \dot{\theta}_b + \dot{\theta}_2 \tag{22a) - (22e}$$

Note that the generalized coordinates and generalized velocities are dimensionless except in time.

Eq. (18) can be written in linear form as:

$$\begin{bmatrix} \dot{\vec{u}} \\ \dot{\vec{q}} \end{bmatrix} = \begin{bmatrix} M^{-1}C & M^{-1}K \\ G & 0 \end{bmatrix} \begin{bmatrix} \vec{u} \\ \vec{q} \end{bmatrix} + \begin{bmatrix} M^{-1}\vec{f} \\ 0 \end{bmatrix} \tag{23}$$

where G is the differential relationship between the generalized coordinates and generalized velocities.

The results are in the state-space form of:

$$\dot{\vec{x}} = A\vec{x} + \vec{x}_o \tag{24}$$

The state vector, $\vec{x}$, is comprised of the generalized velocities, u's, and generalized coordinates, q's.

After the A-matrix is determined, one can examine its eigenvalues for dynamic stability analysis, investigate control issues, and conduct computer simulations.

Symmetric Spacecraft

Although the equations are valid and complete for linear analysis of any hub-arm spacecraft, important phenomenon can be investigated with a simple spacecraft configuration. The symmetry will also aid in finding analytic stability solutions. In particular, a symmetric 2-boom and 4-boom spacecraft will be examined.

Figs. 4a and 4b illustrate these spacecraft. The booms have identical length, mass, surface, and spring properties and are oriented at an angle θ_o. The connection point of the booms to the body is located on the body's centerline at a distance r from the center of gravity.

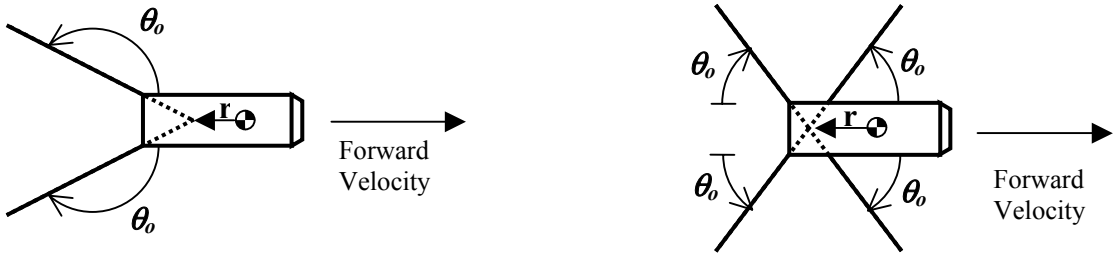

Figs. 4 (a) and (b): Symmetric, 2-Boom and 4-Boom Spacecraft

Non-Dimensionalization

The physical properties of the spacecraft will be non-dimensionalized. Equations with non-dimensional parameters will make the results applicable to a wide range of spacecraft properties.

The basis of the non-dimensionalization is chosen to consist of the following properties:

L^* length of the spacecraft body
m_{tot} mass of the entire spacecraft
S^* cross-sectional surface area of the spacecraft body

V_o spacecraft's orbit velocity
ρ atmospheric density

The non-dimensional properties are:

k boom spring constant (normalized by $1/2\ \rho\ V_o^2\ S^*\ L^*$)
b damping constant (normalized by $1/2\ \rho\ V_o\ S^*\ L^{*2}$)
m mass of each boom (normalized by m_{tot})
r location of boom connection point, $\vec{r}_B$ (normalized by L^*)
x_{AC} location of aerodynamic center (normalized by L^*)
L length of each boom (normalized by L^*)
S surface area of each boom (normalized by S^*)

Two-boom Symmetric Spacecraft

For the two-boom symmetric spacecraft it can be shown[13] that Eq. (24) is in the form:

$$\begin{bmatrix} \dot{u}_1 \\ \dot{u}_2 \\ \dot{u}_3 \\ \dot{u}_4 \\ \dot{u}_5 \\ \dot{q}_1 \\ \dot{q}_2 \\ \dot{q}_3 \\ \dot{q}_4 \\ \dot{q}_5 \end{bmatrix} = -\frac{1}{2}\frac{\rho V_o^2 S^*}{m_{tot} L^*} \left\{ \begin{bmatrix} a_{11} & a_{12} & 0 & a_{14} & -a_{14} & 0 & 0 & a_{18} & a_{19} & -a_{19} \\ 0 & a_{22} & a_{23} & a_{24} & a_{24} & 0 & 0 & a_{28} & a_{29} & a_{29} \\ 0 & a_{32} & a_{33} & a_{34} & a_{34} & 0 & 0 & a_{38} & a_{39} & a_{39} \\ a_{41} & a_{42} & a_{43} & a_{44} & a_{54} & 0 & 0 & a_{48} & a_{49} & a_{59} \\ -a_{41} & a_{52} & a_{43} & a_{54} & a_{44} & 0 & 0 & a_{58} & a_{59} & a_{49} \\ a_{61} & 0 & 0 & 0 & 0 & 0 & 0 & 0 & 0 & 0 \\ 0 & a_{61} & 0 & 0 & 0 & 0 & 0 & 0 & 0 & 0 \\ 0 & 0 & a_{83} & 0 & 0 & 0 & 0 & 0 & 0 & 0 \\ 0 & 0 & a_{83} & -a_{83} & 0 & 0 & 0 & 0 & 0 & 0 \\ 0 & 0 & a_{83} & 0 & -a_{83} & 0 & 0 & 0 & 0 & 0 \end{bmatrix} \begin{bmatrix} u_1 \\ u_2 \\ u_3 \\ u_4 \\ u_5 \\ q_1 \\ q_2 \\ q_3 \\ q_4 \\ q_5 \end{bmatrix} + \begin{bmatrix} x_1 \\ 0 \\ 0 \\ x_4 \\ -x_4 \\ 0 \\ 0 \\ 0 \\ 0 \\ 0 \end{bmatrix} \right\} \tag{25}$$

The details of this derivation can be found from Ref. 13. Each of the a-coefficients in the A-matrix are long and complex expressions of the non-dimensional properties. A mathematical symbolic solver is required to find the exact expression for each a and x coefficient. For numerical solutions, though, the coefficients are simple to calculate.

Four-boom Symmetric Spacecraft

Similarly[13], the four-boom symmetric spacecraft Eq. (24) is in the form:

$$\begin{bmatrix} \dot{u}_1 \\ \dot{u}_2 \\ \dot{u}_3 \\ \dot{u}_4 \\ \dot{u}_5 \\ \dot{u}_6 \\ \dot{u}_7 \\ \dot{q}_1 \\ \dot{q}_2 \\ \dot{q}_3 \\ \dot{q}_4 \\ \dot{q}_5 \\ \dot{q}_6 \\ \dot{q}_7 \end{bmatrix} = -\frac{1}{2}\frac{\rho V_o^2 S^*}{m_{tot} L^*} \left\{ \begin{bmatrix} a_{11} & a_{12} & 0 & a_{14} & -a_{14} & a_{14} & -a_{14} & 0 & 0 & a_{17} & a_{18} & -a_{18} & a_{19} & -a_{19} \\ 0 & a_{22} & a_{23} & a_{24} & a_{24} & a_{26} & a_{26} & 0 & 0 & a_{27} & a_{28} & a_{28} & a_{29} & a_{29} \\ 0 & a_{32} & a_{33} & a_{34} & a_{34} & a_{36} & a_{36} & 0 & 0 & a_{37} & a_{38} & a_{38} & a_{39} & a_{39} \\ a_{41} & a_{42} & a_{43} & a_{44} & a_{54} & a_{64} & a_{74} & 0 & 0 & a_{47} & a_{48} & a_{58} & a_{49} & a_{59} \\ -a_{41} & a_{52} & a_{43} & a_{54} & a_{44} & a_{74} & a_{64} & 0 & 0 & a_{57} & a_{58} & a_{48} & a_{59} & a_{49} \\ a_{41} & a_{62} & a_{63} & -a_{54} & a_{74} & a_{55} & -a_{64} & 0 & 0 & -a_{57} & -a_{58} & a_{78} & a_{69} & -a_{49} \\ -a_{41} & a_{72} & a_{63} & a_{74} & -a_{54} & -a_{64} & a_{55} & 0 & 0 & -a_{47} & a_{78} & -a_{58} & -a_{49} & a_{69} \\ a_{81} & 0 & 0 & 0 & 0 & 0 & 0 & 0 & 0 & 0 & 0 & 0 & 0 & 0 \\ 0 & a_{81} & 0 & 0 & 0 & 0 & 0 & 0 & 0 & 0 & 0 & 0 & 0 & 0 \\ 0 & 0 & a_{93} & 0 & 0 & 0 & 0 & 0 & 0 & 0 & 0 & 0 & 0 & 0 \\ 0 & 0 & a_{93} & -a_{93} & 0 & 0 & 0 & 0 & 0 & 0 & 0 & 0 & 0 & 0 \\ 0 & 0 & a_{93} & 0 & -a_{93} & 0 & 0 & 0 & 0 & 0 & 0 & 0 & 0 & 0 \\ 0 & 0 & a_{93} & 0 & 0 & -a_{93} & 0 & 0 & 0 & 0 & 0 & 0 & 0 & 0 \\ 0 & 0 & a_{93} & 0 & 0 & 0 & -a_{93} & 0 & 0 & 0 & 0 & 0 & 0 & 0 \end{bmatrix} \begin{bmatrix} u_1 \\ u_2 \\ u_3 \\ u_4 \\ u_5 \\ u_6 \\ u_7 \\ q_1 \\ q_2 \\ q_3 \\ q_4 \\ q_5 \\ q_6 \\ q_7 \end{bmatrix} + \begin{bmatrix} x_1 \\ 0 \\ 0 \\ x_4 \\ -x_4 \\ x_4 \\ -x_4 \\ 0 \\ 0 \\ 0 \\ 0 \\ 0 \\ 0 \\ 0 \end{bmatrix} \right\} \tag{26}$$

Note that the a- and x-coefficients in this A-matrix are not necessarily the same as those for the two-boom case.

Spacecraft Body

The boom's aerodynamic coefficients of C_{Do}, C_{Lo}, $C_{D\alpha}$, and $C_{L\alpha}$ are not the only aerodynamic coefficients required in the equations of motion. The spacecraft body's aerodynamic coefficients for drag, lift, and moment are also important. These coefficients can also be expressed linearly as:

$$C_{Db} = C_{Dbo} + C_{Db\alpha}\alpha_b \qquad C_{Lb} = C_{Lbo} + C_{Lb\alpha}\alpha_b \qquad C_{Mb} = C_{Mbo} + C_{Mb\alpha}\alpha_b \qquad (27) - (29)$$

where α_b is the angle of attack of the spacecraft.

Many of the techniques for finding the drag and lift coefficients for the body were discussed previously, but the body's moment slope coefficient $C_{Mb\alpha}$ is an important stability parameter that needs to be examined more closely.

For a symmetric body shape it is known that there will be no net lift produced at a zero angle of attack. Additionally, there will be no net moment produced. Under these conditions, it can be shown[13] that:

$$C_{Mb\alpha} = (C_{Dbo} + C_{Lb\alpha})x^*_{ac} \qquad (30)$$

Since the body drag coefficient and lift-slope curve at zero angle of attack is known or can be calculated, there is a direct relationship between the body's moment-slope coefficient and aerodynamic center. The two can be used interchangeably.

From Anderson[17] or Etkin[18], a stable body in an aerodynamic flow has its aerodynamic center behind the center of gravity. A stable body in this centroid-symmetric shape with no booms has a negative x_{ac}. The term C_{Dbo} is always positive and $C_{Lb\alpha}$ is usually positive for most spacecraft shapes but smaller than C_{Dbo}, so their sum is positive. Then, by Eq. (30), if $C_{Mb\alpha}$ is negative, the body is statically stable. If $C_{Mb\alpha}$ is positive, the body is statically unstable.

Adding booms to the spacecraft will change the stability criteria. Still, the body's moment slope coefficient, $C_{Mb\alpha}$, will play a large role in overall spacecraft stability. As will be seen in the following chapters, any particular boom configuration will impose a requirement on $C_{Mb\alpha}$ that must be met for the entire spacecraft to be stable.

DYNAMIC STABIILTY SOLUTIONS

All of the properties of the booms - mass, size, position, and location - will influence the dynamic stability of the spacecraft. Boom properties will also impose conditions on the spacecraft's body that must be met for stability. By finding analytic stability equations, a spacecraft designer will have a better feel for how to meet these stability conditions.

Given a main body without extra stabilizing characteristics, it would be expected that a rearward-positioned, rearward-facing boom configuration would be stable and a forward-positioned, forward-facing boom configuration would be unstable. It is the same expectation that shooting an arrow with its tail feathers in the back produces nice, stable flight, but shooting it with the feathers in the front will cause erratic, unstable behavior. To see if this is true, an eigenvalue analysis can be conducted for various boom configurations. One can determine stability by calculating the eigenvalues of the A-matrix in Eq. (25) or (26). If all of the eigenvalues are negative, then the system is stable. If there is one or more positive eigenvalues in the group, then the system is unstable.[19] The goal is to derive an analytic solution that will predict the existence of positive eigenvalues and thus the stability of a spacecraft design.

Stability Solutions

Finding the eigenvalues of a large matrix can be easily accomplished numerically with standard software packages. By generating the value of the determinant of the A-matrix (where, in this equation, I is the identity matrix):

$$\det(\lambda I - A) = 0 \qquad (31)$$

a 10th-order polynomial is produced, and solving for λ provides the eigenvalues.

The polynomial also can be reduced to 6th order if the translational eigenvalues are removed. Because there are no horizontal or vertical constraints on the spacecraft, there is no preferred horizontal or vertical position. Therefore, the A-matrix will always have at least two eigenvalues of zero corresponding to the rigid body position modes of the spacecraft. There are also two eigenvalues corresponding to the velocity of the spacecraft. Since the maintenance of stable orbits is not being considered in this analysis, the translational eigenvalues will be ignored when determining the existence of the non-negative eigenvalues for the rotational and vibrational instabilities.

Determining the eigenvalues analytically, however, is both computationally intensive and difficult. The process can be greatly simplified if one only considers whether the eigenvalues are positive or negative, not their exact values. Routh's

stability criteria[20] can be used for such cases. Although features like settling time or peak amplitude won't be determined, at least the designer can see the dividing line between the stable and unstable spacecraft configurations.

By using Routh's stability criteria on this 6th order polynomial, the exact solution of the 6th-order polynomial can be avoided completely. Instead, several smaller inequalities are generated that need to be satisfied. Out of the 6 inequalities that need to be satisfied, 5 are consistently satisfied with realistic spacecraft parameters. However, one of these inequalities is satisfied with only a certain set of spacecraft parameters. It is this inequality that determines the stability and provides an analytic solution to the stability problem. It can be shown[13] that if the following inequality is satisfied by the following A-matrix coefficients for the two-boom case the spacecraft is stable:

(2-boom case)
$$(a_{38}a_{49} - (a_{48} + a_{58})a_{39}) > 0 \tag{32}$$

Finding the eigenvalues for the four-boom solution requires solving a 14th order polynomial. The same analysis, however, can be done as in the two-boom case, and a similar inequality is derived for the four-boom case:

(4-boom case)
$$a_{37}a_{48}a_{69} - (a_{47} + a_{57})(a_{38}a_{69} - a_{48}a_{39}) < 0 \tag{33}$$

The coefficients in this equation are those for the four-boom A-matrix. In both cases, these *a*-coefficients are lengthy expressions determined from carrying out the matrix multiplication in Eq. (23).

6.1.2 Stability Solutions

Substituting in the appropriate expressions into the inequality equations will produce rather lengthy expressions; however, it can be simplified if a couple of assumptions are made. The assumptions are that the mass of the booms is small, and the effective aerodynamic surface area of the booms is reasonably large, i.e.:

$$m << 1 \qquad \frac{S}{mC_{Dbo}} >> 1 \tag{34}$$

Under these assumptions, the result of Eq. (32) can be expanded and rearranged to:

(2-boom case)
$$\frac{C_{Mb\alpha}}{SL} < \frac{-\left(\left(\frac{2k}{SL} - \frac{2r}{L}C_{Do}\right)((C_{D\alpha} - C_{Lo})s_{\theta o} + (C_{L\alpha} + C_{Do})c_{\theta o}) + \frac{2r}{L}\frac{2k}{SL}(C_{L\alpha} + C_{Do})\right)}{\left(\frac{2k}{SL} - (C_{D\alpha} - C_{Lo})s_{\theta o} + (C_{L\alpha} + C_{Do})c_{\theta o}\right)} \tag{35}$$

Similarly, the stability expression can be derived for the four-boom spacecraft configuration under the same assumptions:

(4-boom case)
$$\frac{C_{Mb\alpha}}{SL} < \frac{-2\left(\left(\frac{2k}{SL} - \frac{2r}{L}C_{Do}\right)((C_{D\alpha} - C_{Lo})s_{\theta o} + (C_{L\alpha} + C_{Do})c_{\theta o})^2 + \frac{2r}{L}\left(\frac{2k}{SL}\right)^2(C_{L\alpha} + C_{Do})\right)}{\left(\left(\frac{2k}{SL}\right)^2 - ((C_{D\alpha} - C_{Lo})s_{\theta o} + (C_{L\alpha} + C_{Do})c_{\theta o})^2\right)} \tag{36}$$

The derivation of both these equations can be found in Reference [13]. The equations show that there is a direct link between the boom parameters - mass, size, flexibility, orientation, and positioning - and the body parameter $C_{Mb\alpha}$. The boom parameters impose a condition on the aerodynamic center of the spacecraft body, via $C_{Mb\alpha}$ from Eq. (30), for the entire spacecraft to be stable. Or, given a set aerodynamic center, the equations can be rearranged to determine what boom parameters are necessary to ensure the entire spacecraft is stable.

Many of these types of trades can be done to understand stability. The following section will discuss several of them.

RESULTS

Unless specified otherwise, the spacecraft and atmospheric parameters in Table 1 will be used to help discuss the stability results. These parameters are representative of the planned GEC spacecraft design that will be discussed next. Under these parameters, all of the assumptions discussed in the development of the analytic dynamic stability equations will be met.

The first study will look at how $C_{Mb\alpha}$ varies with boom location and orientation for stability. To simplify the study, the spring constant, *k*, will be set to a very large value (infinity) to simulate a rigid vehicle. This will show how the boom orientation and location normally play a role in stability. Later, *k* will be shown for various values to show what role boom flexibility plays in stability.

Table 1 Nominal Spacecraft Parameters

Variable	Value
L^*	5.0 m
L	2.0
S^*	1.0 m^2
S	0.2
k	4.0
r	–0.5
C_{Dbo}	3.0
$C_{Lb\alpha}$	0.5
ε	0.2
ξ	0.1
$\bar{c} / V_o$	0.1

Stability of a Two-Boom Spacecraft

With k fixed at a large value for rigidity, Fig. 5a shows the stability for various values of $C_{Mb\alpha}$, boom location, and boom orientation. Any value of $C_{Mb\alpha}$ above a designated line in Fig. 5a produces an unstable configuration, while any value of $C_{Mb\alpha}$ below a designated line produces a stable spacecraft configuration. Basically, with a given boom orientation and location, the spacecraft body will need to be designed to have its $C_{Mb\alpha}$ lie below the appropriate line in order for the entire spacecraft to be stable.

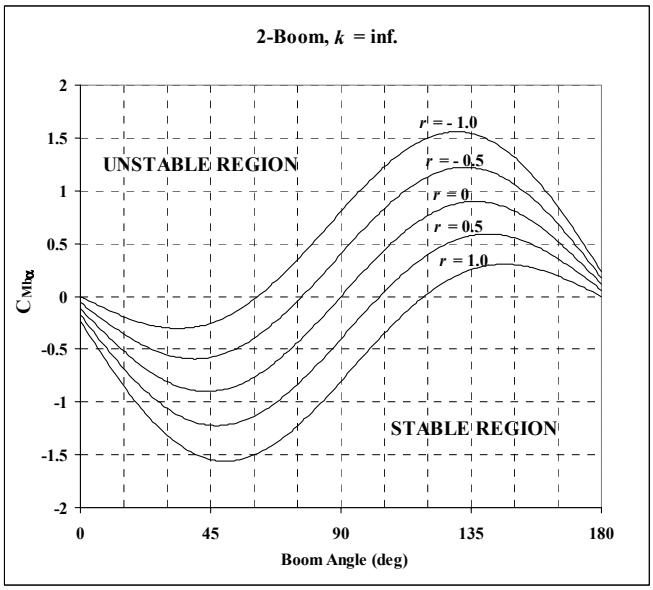

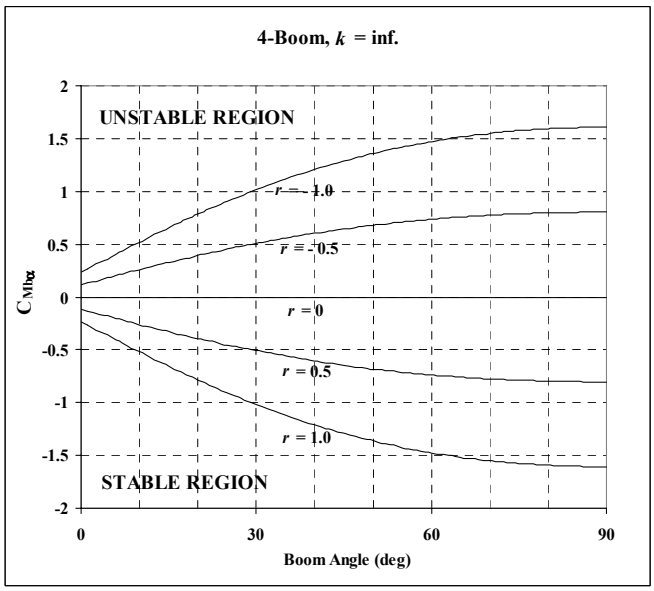

Figs. 5 (a) and (b): Stability Line for Different Boom Locations, 2-Booms and 4-Booms, Rigid

As seen in the figure, a spacecraft with booms located near the front of the spacecraft (positive r values) tends to be less stable than one with booms located near the rear of the spacecraft (negative r values). Additionally, spacecraft with forward-angled booms (0-90 deg) generally tend to be less stable than those with rearward-angled booms (90-180 deg). This means that a spacecraft with forward-facing booms near the front of the spacecraft will require a much more stable spacecraft body design (larger negative $C_{Mb\alpha}$) than a spacecraft with booms near the rear and/or rearward facing booms.

However, since this study concerns itself with flexible boom structures, it is important to look at how flexibility plays a role in stability. With r fixed at 0 for simplicity, Fig. 6a shows how $C_{Mb\alpha}$ changes as k is varied to see what effect the boom stiffness plays in stability. (Note: similar graphs are produced for all ranges of r, except the results are translated up and down similar to Fig. 5a.)

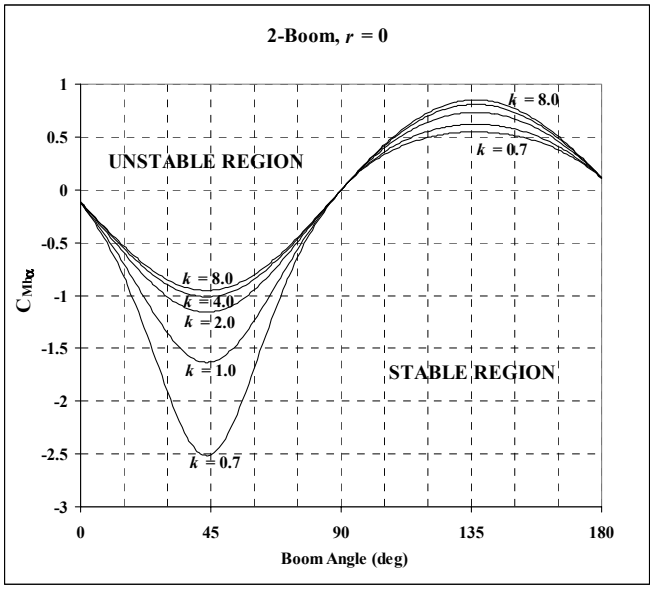

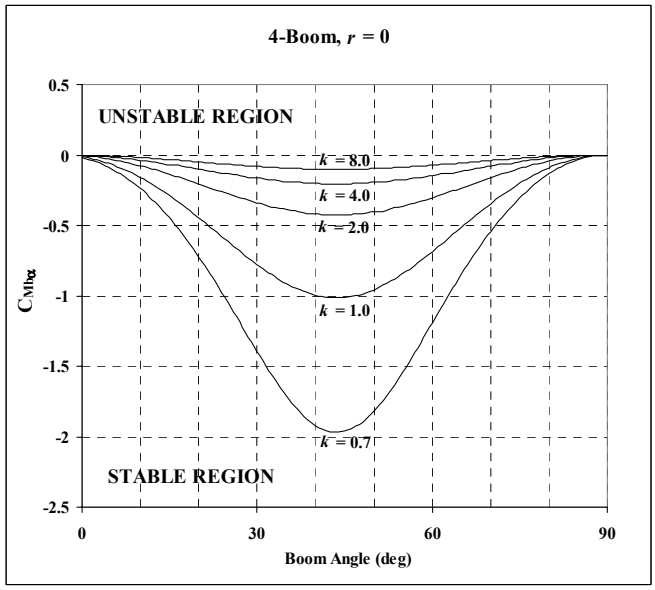

Figs. 6 (a) and (b): Stability Line for Different Spring Constants, 2-Booms and 4-Booms, $r = 0$

In general, the stiffer the boom, the more stable a spacecraft will be. Booms with a lower spring constant tend to destabilize the spacecraft. This effect is most pronounced when the booms are forward-facing as compared to when they are rearward-facing.

It is interesting to note that at a few boom angles, the $C_{Mb\alpha}$ stability line is the same for all ranges of boom spring constants. This occurs near 0, 90, and 180 deg (these are the locations at all ranges of r, too). This is because the aerodynamic forces that produce a moment at the spacecraft body through the spring don't change (linearly) when the boom angle changes slightly from these positions. Therefore, the $C_{Mb\alpha}$ contribution of the booms to the overall spacecraft stability is 0 and is independent of the boom stiffness. The stability requirements change the most near 45 and 135 degrees because the aerodynamic moment has the greatest variance here as the boom angle changes. This moment change modifies the effective spring constant of the boom the most at these points, and hence the stability is affected the most.

It is also seen that the forward-facing booms are more sensitive to changes in k than rearward-facing booms. By examining the denominator of Eq. (35) or (36), one can see that the aerodynamic moment of the booms either adds or subtracts from spring constant. For forward-facing booms, the spring constant is effectively lowered; for rearward-facing booms, the spring constant is effectively increased. The aerodynamic moment is usually small compared to the spring moment, but if the spring moment is also small, the resulting difference between the two orientations is pronounced. Hence, it is easier to destabilize a spacecraft with forward-facing booms when the booms are very flexible.

Finally, it might be assumed that there is a correlation between boom deflection amounts and stability. Certainly, both depend on the value of k, but the correlation isn't direct. The largest boom deflections occur near 90 deg boom orientations where a larger boom surface area is exposed, however that is not where the largest stability differences occur with changing k. It is how the aerodynamic moments change the effective spring constant and not the boom deflections directly that determines stability.

Stability of a Four-Boom Spacecraft

Similar analysis can be done for a spacecraft with four booms. With k fixed at a large value for rigidity, Fig. 5b shows the stability for various values of $C_{Mb\alpha}$, boom locations, and boom orientations for a 4-boom spacecraft. As with the 2-boom spacecraft, a 4-boom spacecraft with booms located near the front of the spacecraft tends to be less stable than one with booms located near the rear of the spacecraft.

With the 4-boom spacecraft, however, there is no net forward-facing or rearward-facing orientation. There are always two booms facing forward and two booms facing rearward. Because of this, when $r = 0$ for a rigid spacecraft, there is no boom angle that is more or less stable than another in the 4-boom configuration. If $r < 0$, then the spacecraft gets more stable as the booms get more perpendicular, but if $r > 0$, then the spacecraft gets less stable as the booms get more perpendicular. Therefore, boom positioning plays more of an interesting role in stability than in the 2-boom case.

As with the 2-boom case, the 4-boom case can also be examined under flexible boom conditions. With r fixed at 0 for simplicity, Fig. 6b shows how $C_{Mb\alpha}$ changes as k is varied to see what effect the boom stiffness plays in stability. Again, booms with a lower spring constant tend to destabilize the spacecraft. The same discussion on the aerodynamic moment produced from the booms also applies. The affect on the spring constant is greatest when the booms are near 45 degrees in the flow with minimal effect when they are at 0 or 90 deg.

Stability of a Six-Boom Spacecraft in Orthogonal Configuration

The 2-boom and 4-boom cases can be combined to investigate the stability of NASA/Goddard's GEC spacecraft. This spacecraft has 6 flexible booms oriented in an orthogonal configuration. An illustration of the spacecraft was shown in Fig. 1. A potential concern is that the booms may cause instabilities.

The same stability equations can be used for the GEC configuration, but this time the boom positions are fixed in an orthogonal arrangement with 4 booms at 45˚ angles in the pitching plane and 2 booms at 90˚ angles in the yawing plane. Because θ_o is fixed for each boom, the design variables x_{AC} and r will be examined instead.

Since the booms of the 6-boom satellite are in different and perpendicular planes, the same equations, Eqs. (35) and (36), can be used as there are two booms in one plane and four in the other plane. See Fig. 7. Because there is no coupling motion in these two planes under our previous assumptions, Eqs. (35) and (36) and can be used independently to find the stability in each plane.

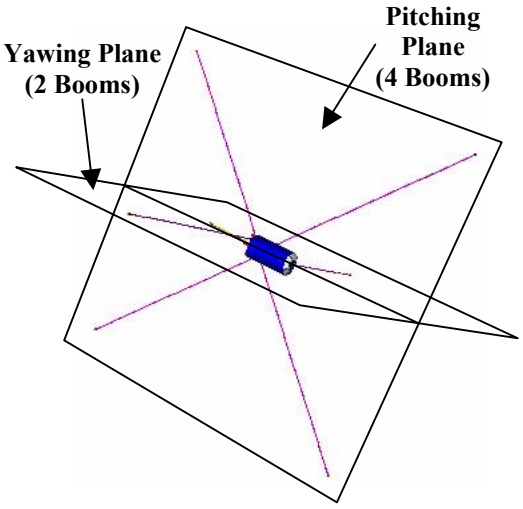

Fig. 7: GEC Pitching and Yawing Planes

The value of C_{Dbo} in Eq. (27), however, needs to be modified to include the drag of those booms not in the plane being examined. In the pitching plane, there are 2 booms that are non-influential "dead weight" as far as that plane is concerned and Eq. (37) applies. In the yawing plane, there are 4 booms that are non-influential "dead weight", and Eq. (38) applies.

$$C_{Mb\alpha} = \left(C_{Dbo} + 2SC_{Do} + C_{Lb\alpha}\right)x_{AC} \qquad C_{Mb\alpha} = \left(C_{Dbo} + 4SC_{Do} + C_{Lb\alpha}\right)x_{AC} \qquad (37), (38)$$

Note: due to the boom's symmetry there is no additional $C_{Lb\alpha}$ modification.

After taking the out-of-plane booms into account, the aerodynamic center location, x_{AC}, was plotted vs. boom location, r, to determine stability in the pitch and yaw planes. (Note that because of the assumed symmetric nature of the spacecraft, x_{AC} is the same for both the pitching and yawing plane.) See Fig. 8.

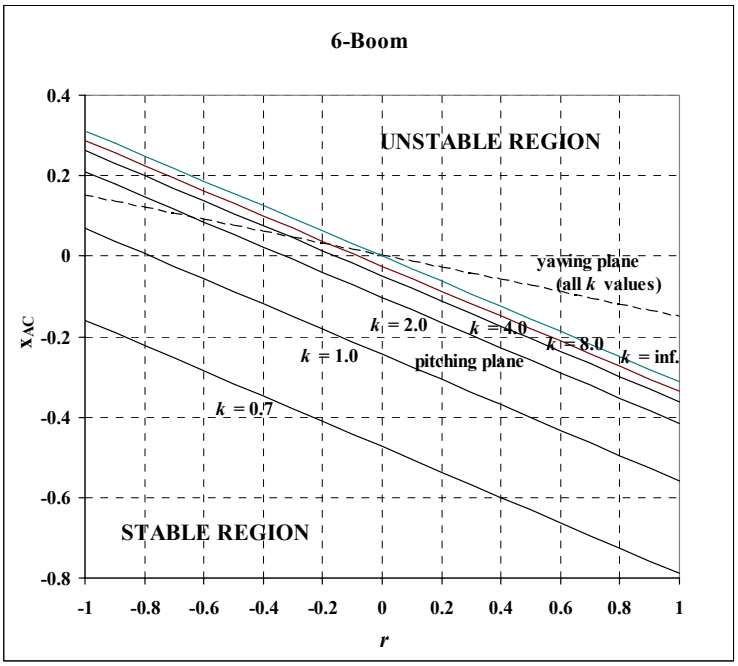

Fig. 8: Stability Line for Different Spring Constants, 6-Booms

The different lines represent the border between the stable and unstable regions with respect to each plane. The solid lines show the separation of the stable and unstable regions for movement in pitching plane for various values of k. The dashed line shows the separation of the stable and unstable regions for movement in the yawing plane. Note that there is only one dashed line. This is because the yaw stability line is independent of the spring constant value when the boom orientation is at 90 degrees as previously discussed. To determine the overall stability of the spacecraft, the lower of the two curves needs to be chosen as the dividing line between the stable and unstable regions.

No matter what the spring constant is, there is always less stability in the pitching plane than the yawing plane for positive values of r. For negative values of r, sometimes the yawing plane is more stable and sometimes the pitching plane is more stable. It depends on the value of the spring constant and the specific negative value of r.

To maintain a stable spacecraft, it is important to choose values of x_{ac} and r that are in the stable region. Note, however, that even if the design parameters of the spacecraft are deemed stable at the beginning of a spacecraft's life, it is possible that they may change over its lifetime. During the spacecraft's mission life, the values of x_{AC} and r could change, say, as fuel is consumed.

Using Fig. 8 as an example, if the fuel was stowed near the front of the spacecraft, as it is consumed, the center of gravity will shift rearward, and the values of x_{AC} and r will become more positive. From any arbitrary initial position in Fig. 8, that point will move up and to the right toward the unstable region.

Finally, if there is any uncertainty in what the exact spring constant of the booms is, near the intersection point it may not be known if the spacecraft becomes unstable first in the pitching plane or the yawing plane. If this is an important consideration, a designer may wish to avoid a configuration that is near this intersection point.

CONCLUSIONS

This work has investigated several different aspects of the dynamics of flexible spacecraft during aeromaneuvers in the rarefied atmosphere. Although the topics of aeromaneuvering, flexible spacecraft dynamics, and rarefied gas flow have separately been examined in the literature, the connection between the three had not been made before. By making this

connection in this work, many important discoveries were made to better understand the behavior of flexible spacecraft during shallow aeromaneuvers. The work also provides a solid basis for further studies.

Analytic Stability Solutions

Most importantly, analytic stability solutions were developed to help a spacecraft builder design a stable spacecraft. The analytic solutions gave much more insight into the physics of the behavior than what the numerical solutions could provide. Simple analytic solutions were found to predict the dynamic stability of the spacecraft.

The analytic dynamic stability solutions provide the most important tool to the spacecraft designer. The solutions give precise recommendations to the designer for ensuring stable flight. The designer can see directly how changes to a spacecraft parameter affect the stability. Flexibility plays an important role in dynamic stability, but its exact role also depends on the orientation and positioning of the booms. The equations also impose requirements on the spacecraft body's center of gravity that must be met for the particular boom properties. The equations can also be used to produce design maps which are useful when tracking stability as the parameters change over the lifetime of the mission.

Application to NASA Missions

Secondly, this work has direct application to the NASA GEC mission spacecraft. This work provides a depth of analysis on stability that hadn't been previously accomplished for this type of atmospheric, dipping mission. The analytic stability solutions developed were modified and applied to this six-boom orthogonal configuration, and several design suggestions resulted from this application. With a given spacecraft body, the booms should be placed as far back on the spacecraft as possible for the greatest stability. Also, making the booms more rigid will also help the stability in the yaw plane, but diminishing returns are seen after a certain level of stiffness.

Also of high importance, the analytic stability solutions provide an easy way to make design trades for the GEC spacecraft. By knowing the relationship of the spacecraft parameters to stability, a designer can see if it is worthwhile to try and improve a specific spacecraft parameter or see if another can be improved more cheaply while still maintaining the same stability result.

Future Work

Now that a foundation has been established to better understand the fundamental dynamics of flexible spacecraft during shallow aeromaneuvers, further studies can be undertaken to refine some of the details or look at new concepts:

1. Future work can be done on improving the gas-surface interaction model. Schultz, Lewis[21] have initially examined how the stability of the spacecraft is influenced by the accuracy of the gas-surface interaction. This work uncovered the need for improved modeling of the gas-surface interaction parameters in order to make better stability predictions. Applying a Nocilla, Cercignani-Lampis, or DSMC rarefied gas model to the analysis could help lower the uncertainty in the lift and drag equations used for stability analysis.
2. Further work can now be undertaken in the area of orbital analysis. The orbital stability and spacecraft stability were separated in this work to concentrate on the spacecraft stability features. Now that the spacecraft stability has been determined, the results can be put into the orbital stability part of the equation to understand the trade off between spacecraft stability and orbital stability.
3. In some applications, pointing accuracy is an important consideration. Now that the equations of motion have been established for this type of spacecraft, work can be done to design control algorithms to achieve pointing accuracies under a changing and unpredictable atmospheric environment.

BIBLIOGRAPHY

[1]Walberg, G. D. "A Survey of Aeroassisted Orbit Transfer", *Journal of Spacecraft and Rockets*, Vol. 22, No. 1, Jan-Feb 1985, pp. 3-18.

[2]Modi, V. J., "Attitude Dynamics of Satellites with Flexible Appendages - A Brief Review", *Journal of Spacecraft and Rockets*, Vol. 11, No. 11, Nov 1974, pp. 743-751.

[3]Hyland, D. C., Junkins, J. L., Longman, R. W., "Active Control Technology for Large Space Structures", *Journal of Guidance, Control, and Dynamics*, Vol. 16, No. 5, Sep-Oct 1993, pp. 801-821

[4]"Understanding Plasma Interactions with the Atmosphere: The Geospace Electrodynamic Connections (GEC) Mission", NASA/TM-2001-209980.

[5]Ketner, G. L., "Survey of Historical Incidences of Controls-Structures Interaction and Recommended Technology Improvements Needed to Put Hardware in Space," Pacific Northwest Lab, PNL-6846/UC-222, March 1989, prepared for Controls-Structures Interaction Office, NASA Langley Research Center.

[6]Moss, J. N., and Bird, G. A., "Direct Simulation of Transitional Flow for Hypersonic Reentry Conditions", AIAA 84-0223, Jan. 1984.

[7]*U.S. Standard Atmosphere, 1976*, NOAA-S/T 76-1562, National Oceanic and Atmospheric Administration, National Aeronautics and Space Administration, United States Air Force, Washington, D.C., Oct 1976.

[8]Maxwell, J. C., "On Stresses in Rarefied Gases Arising from Inequalities of Temperature", Philos. Trans. Royal Society Part I, 1879; reprinted in: *The Scientific Papers of James Clark Maxwell: Volume 2, 1862-1873*, Cambridge University Press, May 1995.

[9]Lewis, M. J., "Aerodynamic Maneuvering for Stability and Control of Low-Perigee Satellites," *Proceedings of the AAS/AIAA Space Flight Mechanics Meeting*, AAS Paper 01-239, Santa Barbara, CA, 11-15 Feb 2001.

[10]Bowman, D. S., Lewis, M. J., "Optimization of Low-Perigee Spacecraft Aerodynamics", *Journal of Spacecraft and Rockets*, Vol. 40, No. 1, Jan-Feb 2003, pp. 56-63.

[11]Bowman, D. S., "Numerical Optimization of Low-Perigee Spacecraft Shapes," Masters Thesis, University of Maryland, College Park, MD, UM-AERO 01-03, 2001.

[12]Sentman, L. H., "Free Molecule Flow Theory and Its Application to the Determination of Aerodynamic Forces", Lockheed Missiles & Space Company, Tech Report LMSC-448514, 1 October 1961.

[13]Schultz, J. R., "Stability of Flexible Spacecraft during Shallow Aeromaneuvers," Doctoral Dissertation, University of Maryland, College Park, MD, 2003.

[14]London, H. S., "Change of Satellite Orbit Plane by Aerodynamic Maneuvering", *Journal of the Aerospace Sciences*, Vol. 29, No. 2, 1962, pp.323-332.

[15]Vinh, N. X., *Optimal Trajectories in Atmospheric Flight*, Elsevier Scientific Publishing Co., New York, NY, 1981.

[16]Stevens, B. L., Lewis, F. L., *Aircraft Control and Simulation*, John Wiley & Sons, Inc., New York, 1992, pp 46-47.

[17]Anderson, J. D., Introduction to Flight, Third Edition, McGraw-Hill, Inc., New York, 1989, pp. 369-374.

[18]Etkin, B., Dynamics of Flight - Stability and Control, John Wiley & Sons, Inc., New York, 1982, pp. 14-15.

[19]Chen, C., *Linear System Theory and Design, Third Edition*, Oxford University Press, New York, 1999, pp. 121-140.

[20]Ogata, K., *Modern Control Engineering, 3rd Edition*, Prentice Hall, Upper Saddle River, NJ, 1997, pp. 232-238.

[21]Schultz, J. R., Lewis, M. J., "Drag and Stability of a Low-Perigee Satellite", 13th AAS/AIAA Space Flight Mechanics Conference, AAS 03-182, Ponce, Puerto Rico, 9-13 Feb 2003.